

Yibin Xu,^{a*} Daying Wen,^{a‡}
Carmen Brown,^a Chun-Jung
Chen,^b Paul D. Carr,^c David L.
Ollis^c and Subhash G.
Vasudevan^{a‡}

^aDepartment of Biochemistry and Molecular
Biology, James Cook University, Townsville,
Queensland 4811, Australia, ^bBiology Group,
Research Division, National Synchrotron
Radiation Research Center, Hsinchu 30077,
Taiwan, and ^cResearch School of Chemistry,
Australian National University, GPO Box 414,
Canberra, ACT, 2601, Australia

‡ Present address: Novartis Institute for Tropical
Diseases Pte Ltd, 1 Science Park Road,
#04-14 The Capricorn, Singapore Science
Park II, Singapore 117528.

Correspondence e-mail: yxu@svi.edu.au

Received 12 November 2004
Accepted 2 June 2005
Online 15 June 2005

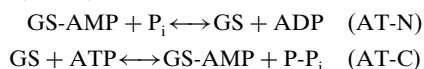
Expression, purification and crystallization of the C-terminal domain of *Escherichia coli* adenylyltransferase

The C-terminal domain of adenylyltransferase (ATase) from *Escherichia coli* has been overexpressed, purified and crystallized in a form suitable for structure analysis. The domain is contained in a fragment that extends from residues 441–945 of the intact ATase.

1. Introduction

Adenylyltransferase (ATase; EC 2.7.7.42) from *Escherichia coli* is a key element of the cascade that regulates the uptake of nitrogen in enteric and other bacteria (Stadtman, 2001). Specifically, it catalyses the adenylylation and deadenylylation of glutamine synthetase (GS), thereby modulating its catalytic activity. The PII protein and effectors such as glutamine and 2-oxoglutarate (2OG) regulate the two antagonistic activities of ATase (Jiang *et al.*, 1998; Ninfa & Atkinson, 2000; Arcondeguy *et al.*, 2001). PII is a signal transduction protein and indicates nitrogen status in most bacteria. In a low-nitrogen environment PII is converted to PII-UMP. In this form, PII binds to ATase as a complex with ATP and 2OG and inhibits the adenylylation activity, at the same time stimulating the deadenylylation activity of ATase. In a high-nitrogen environment, unmodified PII and glutamine bind to ATase, with a consequent reduction in deadenylylation activity and an activation of adenylylation activity.

The two catalytic activities of ATase reside in distinct domains. The C-terminal domain, designated AT-C, is responsible for the adenylylation activity, while the N-terminal domain, designated AT-N, is responsible for the deadenylylation activity (Jaggi *et al.*, 1997). The reactions catalyzed by these two domains are somewhat similar,



Both domains show sequence similarity to enzymes with the β -polymerase fold, although structural analysis of the AT-N domain revealed that this similarity was limited to a small section of the active site and that even some of the secondary-structure elements within the active site were linked in a different manner to other polymerases (Xu, Zhang *et al.*, 2004). Although the two domains can catalyze the reactions of ATase separately, they lack most of the regulatory capacity of the intact molecule (Jaggi *et al.*, 1997). While the intact ATase has proven to be very difficult to crystallize, the individual domains from constructs of various lengths have yielded crystals. The suitability of these crystals for structural analysis depended on the lengths of the fragments. In a previous study, we described the reasoning that led to the identification of stable and soluble N-terminal domain, AT-N440, that could be readily purified and crystallized (Xu, Wen *et al.*, 2004). Attempts to crystallize C-terminal fragments generated in a previous study (Jaggi *et al.*, 1997) led to only limited success. For example, we purified and crystallized AT-C517 consisting of residues 429–945. Although the crystals were large, they only diffracted to about 4.5 Å in a synchrotron beam. It was noted that AT-C517 contained 12 residues that were present in the AT-N440 fragment. The peptide in question formed half of the final helix of AT-N440. By removing these 12 residues, a domain that was more suitable for structure analysis was obtained. Here, we report the

cloning, expression, purification and crystallization of AT-C505, which covers the 505 residues from 441 to 945 of the full-length ATase.

2. Materials and methods

2.1. Cloning, expression and purification

The appropriate region of *glnE* was amplified by the polymerase chain reaction (PCR SuperMix High Fidelity, Invitrogen) to give the fragment encoding C-terminal truncations AT-C505 which starts from the Q1 linker of ATase (forward primer AT-C505FP, 5'-GATATACATATGAGTGAACTCAGGAAGAG-3'; reverse primer M13 universal primer, 5'-TGTAACAACGACGGCCAGT-3'). The *glnE* gene in the pRJ009 plasmid was used as the template (Jaggi *et al.*, 1997). The pRJ009 plasmid was constructed by using the thermo-inducible expression vector pND707 with the strong λ P_LP_R promoter (Love *et al.*, 1996). The forward primer introduced *Nde*I sites and placed an ATG start codon for the translation of construct at the beginning of the PCR fragment. The PCR product was digested with *Nde*I and *Sph*I and the resulting fragment was inserted into the same site of the digested pRJ009. The resulting plasmid pAT-C505 directed the synthesis of the truncated protein AT-C505. The correctness of the clone was confirmed by nucleotide sequence analysis.

The plasmid pAT-C505 was used for high-level heat-inducible expression of AT-C505 in *E. coli* strain JM109 in Luria–Bertani broth (LB) containing 100 $\mu\text{g ml}^{-1}$ ampicillin at 303 K with shaking until OD₅₉₅ reached ~ 0.5 . Cultures were induced by raising the temperature quickly to 315 K. Growth was continued for a further 3 h. The resulting cells were pelleted by centrifugation in an Avanti centrifuge (Beckman Coulter) at 8000g for 10 min. These pellets were resuspended in lysis buffer (20 mM Tris–HCl pH 8.0, 1 mM MgCl₂, 1 mM PMSF, 0.1 mM pepstatin, 0.1 mM leupeptin and 5 mM β -mercaptoethanol) and lysed with a French pressure cell (Aminco). Cell debris was removed by centrifugation at 40 000g for 30 min.

The purification of AT-C505 was carried out using the same protocol as for AT-N440 (Xu, Wen *et al.*, 2004). Ground ultrapure (NH₄)₂SO₄ was added to the supernatant to 25%(w/v) saturation. The protein solution was centrifuged at 40 000g for 30 min to remove precipitated material. Following centrifugation, (NH₄)₂SO₄ was added to 60%(w/v) saturation. The precipitated protein was resuspended in 50 ml buffer A (20 mM Tris pH 8.0, 1 mM MgCl₂ and 5 mM β -mercaptoethanol) containing 20%(w/v) ammonium sulfate. The protein solution was then loaded onto a Phenyl-Sepharose High Performance (Amersham) column equilibrated with buffer A containing 20%(w/v) ammonium sulfate. The column was washed with 200 ml buffer A containing 20% ammonium sulfate followed by a 500 ml reverse linear gradient (from 20 to 0%) of ammonium sulfate in buffer A. AT-C505 was eluted at about 8% ammonium sulfate. The peak fractions from the hydrophobic interaction chromatography step were characterized by SDS gels, pooled together, diluted fivefold with buffer A to about 50 mM ammonium sulfate and loaded onto a Source 15Q anion-exchange column (Amersham) which had been previously equilibrated with buffer A. The protein was eluted from the Source 15Q column at 300–350 mM NaCl with a 0–1 M NaCl gradient in buffer A. The peak fractions were pooled and concentrated to ~ 1.5 ml. The concentrated AT-C505 sample was loaded onto a Superdex 200 gel-filtration column (Amersham) pre-equilibrated with buffer B (20 mM Bis-Tris pH 6.5, 150 mM NaCl, 1 mM MgCl₂ and 5 mM β -mercaptoethanol). Fractions containing AT-C505 were pooled and concentrated to 16 mg ml⁻¹. The final

Table 1

Data-collection statistics.

Values for the highest resolution shell are given in parentheses.

Space group	<i>P</i> 2 ₁ 2 ₁ 2 ₁	<i>P</i> 2 ₁ 2 ₁ 2 ₁
Unit-cell parameters		
<i>a</i> (Å)	72.54	72.96
<i>b</i> (Å)	122.86	133.90
<i>c</i> (Å)	143.62	135.07
$\alpha = \beta = \gamma$ (°)	90	90
Resolution (Å)	2.40 (2.49–2.40)	2.80 (2.90–2.80)
Observed reflections	752649	791207
Unique reflections	49185	32967
Completeness (%)	96.4 (93.8)	100 (100)
<i>R</i> _{merge} † (%)	8.9 (49.2)	7.2 (46.1)
<i>I</i> / σ (<i>I</i>)	8.4 (3.2)	12.9 (5.0)
Redundancy	3.0	7.6
Mosaicity (°)	0.55	0.71

$$\dagger R_{\text{merge}} = \sum I - \langle I \rangle / \sum I.$$

AT-C505 protein was stored in 20 mM Bis-Tris pH 6.5, 1 mM MgCl₂ and 5 mM β -mercaptoethanol for crystallization trials.

2.2. Crystallization

AT-C505 was crystallized by the hanging-drop vapour-diffusion method at 277 K from drops containing 3 μl protein and 2 μl reservoir solution equilibrated against 1 ml reservoir solution consisting of 2 M ammonium sulfate, 0.1 M Tris pH 8.0 or 8.5. Crystals appeared after one week and reached maximum size in two weeks. The diffraction-quality crystals were used for X-ray data collection.

2.3. Data collection and processing

The protein crystals were initially screened and characterized using synchrotron radiation from the protein crystallographic beamline BL17B2 equipped with a MAR345 imaging-plate detector (Rigaku/MSI Inc.) at the National Synchrotron Radiation Research Center (NSRRC) in Taiwan. The further complete data collection was carried out at BL12B2 equipped with a Quantum-4R CCD (ADSC) detector at SPring-8 in Japan. The crystal was transferred into cryo-protectant solution containing 30% sucrose, mounted in a 0.2–0.3 mm glass loop (Hampton Research) and flash-cooled in liquid nitrogen at 100 K. For a complete data set, contiguous 1° oscillation images were collected for a total crystal rotation of 180° using a wavelength of 1.00 Å with an exposure time of 40 s and a crystal-to-detector distance of 200 mm. The crystal was maintained at 100 K in a nitrogen stream using the X-Stream cryo-system (Rigaku/MSI, Inc.). The data were indexed, integrated, scaled and merged using the program *HKL2000* (Otwinowski & Minor, 1997). Details of the data statistics are given in Table 1.

3. Results and discussion

AT-C505 crystals of rectangular shape were visible in one week and continued growing to maximum dimensions of 0.1 \times 0.1 \times 0.3 mm in four weeks at 277 K. Crystals suitable for data collection were identified and were found to exhibit orthorhombic symmetry. Interestingly, two crystal forms with different unit-cell parameters were observed from the same crystallization conditions: *a* = 72.54, *b* = 122.86, *c* = 143.62 Å and *a* = 72.96, *b* = 133.90, *c* = 135.07 Å. Systematic absence suggested that both crystals belong to space group *P*2₁2₁2₁. These two data sets were 96.4 and 100% complete, with internal agreements (*R*_{sym}) of 8.9 and 7.2% for the resolution range 25.0–2.40 and 25.0–2.80 Å, respectively. Assuming the presence

of two molecules per asymmetric unit, the Matthews coefficient is estimated to be $2.8 \text{ \AA}^3 \text{ Da}^{-1}$, corresponding to a solvent content of about 55% for both crystal forms, which is within the normal range for protein crystals. The determination of structures by MAD phasing is under way.

We are grateful to the beamline support staff, Yu-Cheng Jean, Yu-San Huang and Chun-Shiun Chao, for excellent technical assistance and discussion of the synchrotron-radiation X-ray facility during data collection at BL17B2 of NSRRC in Taiwan and at BL12B2 of SPring-8 in Japan.

References

- Arcondeguy, T., Jack, R. & Merrick, M. (2001). *Microbiol. Mol. Biol. Rev.* **65**, 80–105.
- Jaggi, R., van Heeswijk, W. C., Westerhoff, H. V., Ollis, D. L. & Vasudevan, S. G. (1997). *EMBO J.* **16**, 5562–5571.
- Jiang, P., Peliska, J. A. & Ninfa, A. J. (1998). *Biochemistry*, **37**, 12802–12810.
- Love, C. A., Lilley, P. E. & Dixon, N. E. (1996). *Gene*, **176**, 49–53.
- Ninfa, A. J. & Atkinson, M. R. (2000). *Trends Microbiol.* **8**, 172–179.
- Otwinowski, Z. & Minor, W. (1997). *Methods Enzymol.* **276**, 307–326.
- Stadtman, E. R. (2001). *J. Biol. Chem.* **276**, 44357–44364.
- Xu, Y., Wen, D., Clancy, P., Carr, P. D., Ollis, D. L. & Vasudevan, S. G. (2004). *Protein Expr. Purif.* **34**, 142–146.
- Xu, Y., Zhang, R., Joachimiak, A., Carr, P. D., Huber, T., Vasudevan, S. G. & Ollis, D. L. (2004). *Structure*, **12**, 861–869.